Organic matter accumulation during the Holocene in the Guadalquivir marshlands (SW Spain)

JOSÉ E. ORTIZ[1]*, TRINIDAD TORRES[1], JOSÉ E. LÓPEZ-PAMO[2], VICENTE SOLER[3], JUAN F. LLAMAS[1], DANIEL BARETTINO[2] and MARÍA J. GARCÍA[1]

[1]*Laboratory of Biomolecular Stratigraphy, E.T.S.I. Minas Madrid, Universidad Politécnica de Madrid, Madrid, Spain*
[2]*Instituto Geológico y Minero de España, Madrid, Spain*
[3]*Instituto de Agrobiología y Productos Naturales (CSIC), La Laguna, Tenerife, Spain*

The distribution of biomarker compounds and magnetic susceptibility observed in the sediment from a 20 m core drilled in the marshlands of the estuarine region of the Guadalquivir River (southwest coast of Spain) has allowed us to reconstruct the palaeoenvironmental evolution of this area during the Holocene. Several organic compounds (*n*-alkanes, *n*-ketones, *n*-alkanols, *n*-alkanoic acids and organic sulphur), as well as different biomarker ratios, have been used to show changing environmental conditions through time. These geochemical proxies suggest good preservation of the organic matter, although some diagenesis has occurred to particular organic compounds, especially the *n*-alkanoic acids. Our data indicate a major allochthonous supply of terrestrial plants, with less influence from aquatic plants or algae through the core. There are markedly different palaeoenvironmental conditions between the uppermost 5 m (last 6 ka cal. B.P.) and the rest of the core. From 5 m (*ca* 6 ka cal. B.P.) to 19 m (*ca* 8 ka cal. B.P.) depth the palaeoenvironmental conditions were almost constant. Based on organic sulphur content and *n*-alkane content logs, anoxic conditions prevailed from 8 to 6 ka cal. B.P., while oxic conditions with enhanced convection of water (prevalence of fluvial input), and consequently a greater organic matter supply, predominated in the upper 5 m of the core. Similarly, little variation in the magnetic susceptibility profile below 5 m indicates stable environmental conditions, while in the upper 5 m conditions shifted to one with elevated water input and clastic sediment supply. This is linked to palaeofloral alterations in the Guadiamar/Guadalquivir drainage basins and/or anthropogenic effects. We propose that from *ca* 8 to 6 ka cal. B.P. a stable landscape physiognomy in the surroundings of the estuarine area of the Guadalquivir River, with a predominance of pines and grassland. However, over the last 6 ka cal. B.P. a variation in the terrestrial plant biomarker compounds suggests an alternation of relatively dry and humid phases and/or the impact of human populations on altering the vegetation community have occurred.

1. INTRODUCTION

After the Last Glacial Maximum, the Holocene marine transgression resulted in the emerged lowlands of the down-valley part of the Guadalquivir River becoming flooded and the riverine environment changing into a marshland (marismas according to the local description; Goy *et al.* 1996; Rodríguez Vidal *et al.* 1997; Dabrio *et al.* 2000). This led to the palaeo-river linked gravel deposition changing into dark coloured mud or very fine-grained sand containing abundant ostracods and pollen as well as some scattered brackish water mollusc shells (Zazo *et al.* 1999; Yll *et al.* 2003; Ruiz *et al.* 2005). Previous studies of the area have focussed not only on the coastal

morphology and its evolution (Zazo *et al.* 1994; Goy *et al.* 1996; Rodríguez Vidal *et al.* 1997; Borja *et al.* 1999), but also on sedimentology (Dabrio *et al.* 2000; Lario *et al.* 2002; Lobo *et al.* 2005; Ruiz *et al.* 2005) and environmental evolution (Zazo *et al.* 1999; Yll *et al.* 2003).

In 1999, a borehole was drilled in the vicinity of Villamanrique (Huelva Province, Andalusia, Spain) at the mouth of the Guadiamar River near its confluence with the Guadalquivir River (Figure 1). Estuarine areas are good environments for studying the origin of sedimentary organic material due to the rapid accumulation of fine-grained sediment, sealing them from bacterial remineralization (Hedges and Keil 1999), this core was sampled for palaeoenvironmental reconstruction purposes.

The main purpose of this study was to determine the origin of the organic matter, the palaeoenvironmental conditions prevailing during the Holocene, and the status of the area before and after any anthropogenic effects, especially from mining. A multidisciplinary study, including sedimentological description, magnetic susceptibility and characterization of the organic matter content, particularly the lipid fraction at a molecular level (biomarkers), of diverse samples taken along the core was carried out. Specifically, metallurgical settlements that were dependent on mining districts (Iberian Pyrite Belt) around alluvial valleys of south-western Iberian Peninsula (Guadalquivir and Guadiana) has been documented for the last 5000 years B.P. (Leblanc *et al.* 2000; Nocete *et al.* 2005).

2. GEOGRAPHICAL AND GEOLOGICAL SETTING

The borehole (20 m-long, 92 cm-width) was drilled in the vicinity of Villamanrique de la Condesa (37°11′7″N, 6°1229″W), close to the confluence of the Guadiamar and the Guadalquivir rivers near the mouth of this latter in the Gulf of Cádiz (Atlantic Ocean; Figure 1). This area is dominated by extensive marshlands, covering 1800 km^2, most of them protected and located within the Doñana National Park and in its north boundary important massive sulphide deposits belonging to the Iberian Pyrite belt are found.

The coast of the Gulf of Cádiz (SW Spain) can be described as a semidiurnal mesotidal one (Borrego *et al.* 1993). These characteristics, together with the coast morphology and the energy (medium) and direction of the waves (south-easterly), favour the development of broad littoral lowlands, usually sheltered by spits, where tidal flats and fresh water marshes extend some kilometres inland.

The Guadalquivir River is one of the longest in Spain, with a total length of 580 km. In its lower course, near the mouth, the substratum consists of soft non-consolidated Plio-Pleistocene sediments. In fact, during the Pliocene and Pleistocene most of this area was covered by the sea and during the late Pleistocene/Holocene the actual river mouth area acted as an extensive marshland with deltaic and alluvial influence, in some cases being this latter dominant, depending mostly on global sea level oscillations (Dabrio *et al.* 2000). Silts and argillaceous sediments are predominant, with some interbedding of sand and gravel. The borehole was situated over dark lutites (mainly silt) deposited in an extensive marshland during the Holocene (Torres 1975; González-Delgado *et al.* 2004). The Guadalquivir marshland is enclosed by natural spits bars which, in the Gulf of Cádiz, were constructed over four episodes (Zazo *et al.* 1994): 6.5–4.7 ka cal. B.P., 4.4–2.7 ka cal. B.P., 2.4–0.7 ka cal. B.P. and the last 500 cal. year.

During the sea level fall linked to the last glacial period, the Guadalquivir river, as well as others that flow into the Gulf of Cádiz, excavated incised valleys. The following rapid sea level rise during the Holocene resulted in the down-valley areas of these rivers evolving into estuaries. In fact, according to different studies (Goy *et al.* 1996; Borrego *et al.* 1999; Dabrio *et al.* 2000) the filling of the estuaries of the Gulf of Cádiz began during the Holocene transgression. During the post-glacial transgression maximum, at 6.5–6 ka cal. B.P. (Zazo *et al.* 1994) the transgressed areas changed from brackish to more open marine and the estuaries reached their maximum surficial extension (Dabrio *et al.* 2000). Afterwards, the estuarine filling followed a twofold pattern characterized by a progressive change from vertical accretion to lateral progradation. At 4 ka cal. B.P. a partial emergence of tidal flats and spit barriers occurred because of important fluvial sediment input. Prevalence of coastal progradation over vertical accretion at 2.4 ka cal. B.P. caused the expansion of tidal flats and the rapid growth of sandy barriers. Further changes reflect anthropogenic impacts and the filling of the estuaries continued to the present day (Goy *et al.* 1996; Dabrio *et al.* 1999, 2000).

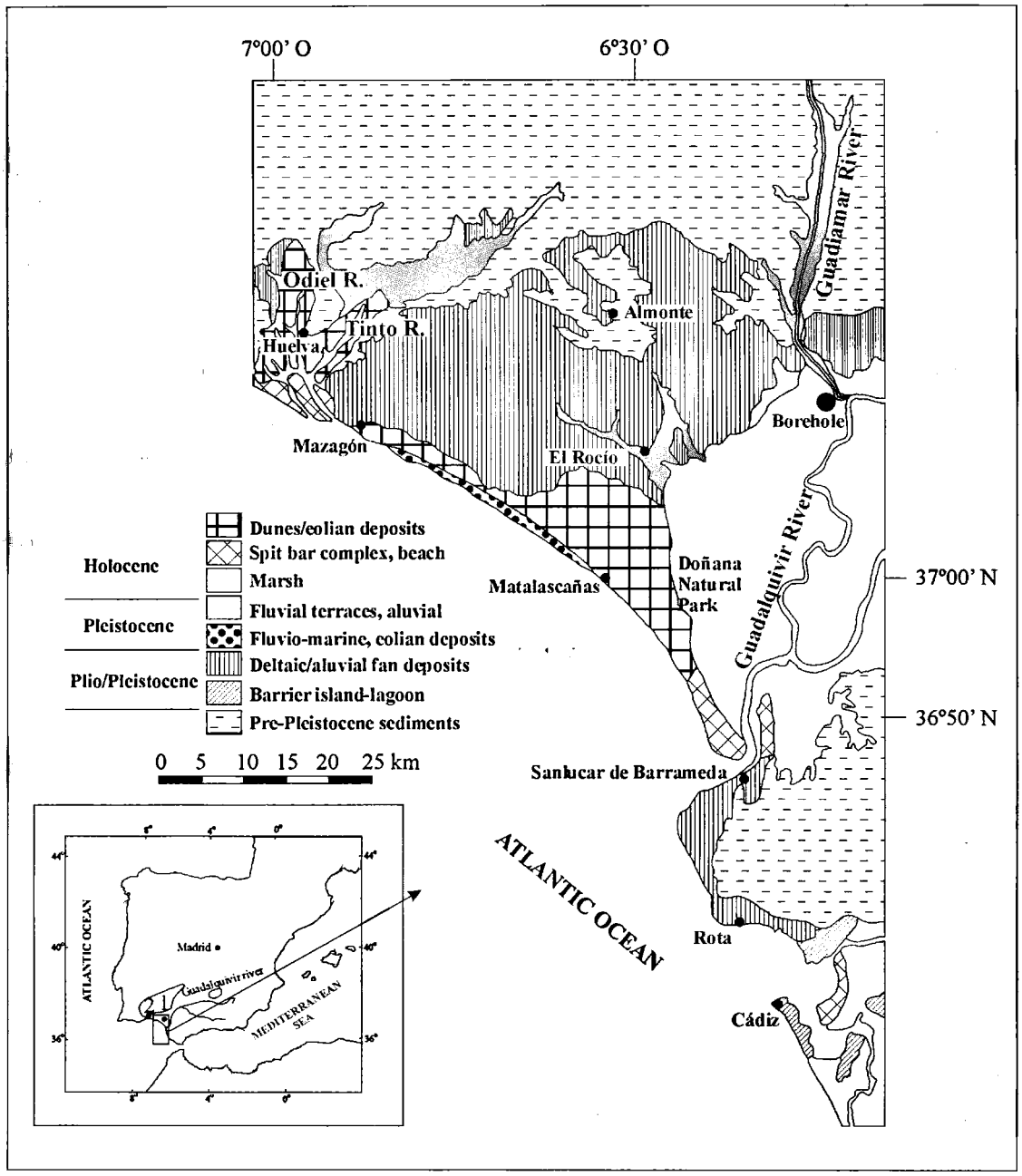

Figure 1. Geography and geology of Gulf of Cádiz region (southwest Spain), with location of the Guadalquivir/Guadiamar estuarine areas (modified from González-Delgado *et al.* 2004). The location of the Villamanrique core (1) is shown on the map of the Iberian Peninsula, along with the core studied by González-Vila *et al.* (2003) in the Guadiana River estuarine area (2). The main sulphide ore deposits are shown in grey.

The mean annual temperature in the area is 16.9°C and the precipitation is 614 mm (Rivas-Martínez and Rivas y Sáenz 2006). According to Yll *et al.* (2003) the vegetation is dominated by Mediterranean scrub in the high zones of the Doñana National Park and by Atlantic-type scrub in the depressions. *Pinus picea*, *Quercus suber*, *Pistacia lentiscus* and *Arbutus unedo* are also present, together with junipers and savins. In some areas (inner dune

depressions) *Armeria arenaria*, *Carex* and *Artemisia campestris* occur. In the salt marshes *Salicornia* and rushes are predominant.

2.1. Borehole description

The stratigraphy of the Villamanrique borehole is presented in Figure 2. It was obtained using a rotary rig equipped with a core barrel that recovered 92 cm diameter cores using a wire-line device. The core recovery was nearly about 100% and fine-grained sands and lutites are the predominant materials, except at the bottom where conglomerates, probably of Pleistocene age appear (20–25 ka B.P., cf. Dabrio *et al.* 2000). In some cases, fossil remains are abundant, especially oysters, *Cardium* sp. and *Barnea* sp., which are typical of intertidal areas. Foraminifera tests and ostracode valves, mainly *Loxoconcha* sp., appear in some horizons, and plant remains are also observed throughout the core and are especially abundant between 14.55 and 13.55 m, 10.95 and 10.15 m and 9.15 and 5.55 m, while pyrite clasts are present between 13.55 and 10.95 m and 9.95 and 9.35 m.

Microfauna and plant remains are very scarce in the uppermost 3.35 m, and some brackish and terrestrial gastropod and pelecypod fragments are the only faunal remains in this zone. Clay and mica grains are very abundant and dominate over quartz and feldspar. Sedimentology and fossils indicate that they were deposited in a brackish muddy marshland (*marisma*), and the pelecypod shells found around 8 m probably reflect the Flandrian flooding event (cf. Zazo *et al.* 1999), coinciding with the maximum in the post-glacial transgression. We refer to the sampled horizons of the borehole by depth, in centimetre, from top to bottom (e.g. sampled level VM-525 is from 525 cm).

3. MATERIALS AND METHODS

The core was split longitudinally in half, photographed and stored frozen at −20°C until required for analysis. Four samples were taken for AMS radiocarbon dating. Some others were taken for lipid analysis and magnetic susceptibility determination.

3.1. AMS radiocarbon dating

AMS radiocarbon dating was undertaken on bulk organic matter of samples VM-120, VM-378, VM-579 and VM-1703, at Beta-Analytic, Inc., Florida, following pre-treatment with dilute HCl to ensure the absence of carbonate. Material measured using the AMS technique was analysed by reducing the sample carbon to graphite (100%). The graphite was then examined for ^{14}C content with an accelerator mass spectrometer, and the radiocarbon age was calculated. The age was calibrated using the INTCAL 98 radiocarbon age calibration program (Stuiver *et al.* 1998).

3.2. Lipid extraction and analysis (biomarker analysis)

A total of 26 samples were taken along the core. About 40–45 g of freeze-dried sediment (at 50°C for 24 h) per sample were grounded and biomarkers were extracted following the Laboratory of Biomolecular Stratigraphy protocol (Lucini *et al.* 2000), which consists of: 24 h soxhlet extraction with dichloromethane and methanol 2:1 (suprasolv Merck) and concentration of the isolated lipid extract using a rotary evaporator. Three lipid extract fractions were obtained using liquid chromatography in a silica-alumina glass column (14.2 g of silica, 7.7 g of alumina; 70–230 mm mesh) using solvents of different polarity (80 ml in all cases): hexane, dichloromethane/hexane 80% and methanol to yield neutral, polar and acid fractions. Prior to analysis in gas chromatograph mass spectrometer (GC-MS), acidic and polar fractions were methlylated with trimethylsilyldiazomethane and silylated with a mixture of N,O-bis(trimethylsilyl) trifluoroacetamide (BSTFA) and pyridine at 70°C for 2 h.

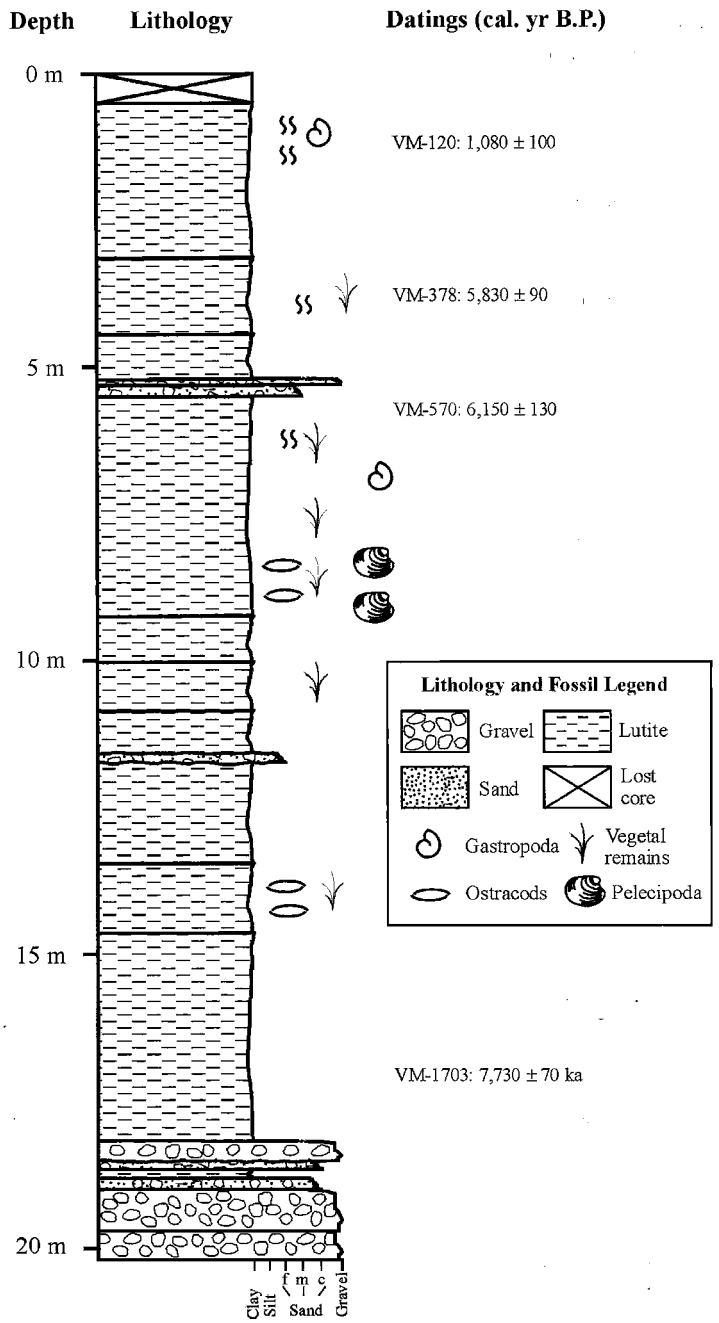

Figure 2. Stratigraphy and chronology of Villamanrique borehole core. Calibrated ages (cal. B.P.) obtained from the radiocarbon method are included.

Samples were injected into an HP 6890 gas chromatograph equipped with a selective mass detector (HP 5973) and an ATM-5 column (250 × 0.25 mm; 0.20 μm). Helium was the carrier gas. The oven temperature was programmed from 60 to 300°C at 6°C/min (hold time 20 min). The injector was maintained at 275°C. Components were identified with the Data Analysis program and the Wiley Library; *n*-alkane distributions were obtained from

the GC/MS chromatograms of m/z 57 in fraction A, *n*-ketones from m/z 58 in fraction B, *n*-alkanols from m/z 83 in fraction C, *n*-alkanoic acids from the m/z 74 in fraction B and organic sulphur from the m/z 64 in fraction A.

3.3. Magnetic susceptibility

The magnetic susceptibility was measured at a resolution of approximately 10 cm intervals using a KLY-2 Kappabridge from AGICO, equipped with the SUFAR software. A total number of 67 samples were taken along the 20 m-long core. The equipment is automatically zeroed and the errors are estimated using the Sufar software based on multivariate statistical analysis. The magnetic susceptibility and its anisotropy can be measured from 3 *A/m* to 450 *A/m* in 21 measurements.

4. RESULTS

4.1. Chronology

The ages are presented in Table 1 and Figure 2. The results show that the borehole covers most of the Holocene. Figure 3 shows dating versus depth assuming a constant sedimentation between points. This enables the age of undated intermediate horizons to be calculated. These results indicate the existence of two distinct phases; the first extends from the bottom of the core to metre 5 (*ca* 8 to *ca* 6 ka cal. B.P.), with a mean sedimentation rate of 7 mm/year, while the second, at the uppermost 5 m (after 6 ka cal. B.P.), yields a mean sedimentation rate of 0.54 mm/year, coinciding with results of Lario *et al.* (2002) for different Holocene estuaries from SW Iberia, including those from the Guadalete, Guadalquivir and Tinto-Odiel rivers.

4.2. n-Alkanes

The logs of the different indexes related to the *n*-alkane content used in this paper, that is the carbon preference index (CPI), *n*-alkane predominant chain, long-chain/short-chain ratio, terrigenous/aquatic ratio, *P*aq index and relative percentages of the C_{27}, C_{29} and C_{31} *n*-alkanes are shown in Figures 4a, 5a and 6a–d.

The CPI (Bray and Evans 1961) represents the predominance of odd over even *n*-alkanes of a certain chain length range and is calculated as the $^1/_2[(\sum C_i + C_{i+2} + \ldots + C_{i+8})/(\sum C_{i-1} + C_{i+1} + \ldots + C_{i+7}) + (\sum C_i + C_{i+2} + \ldots + C_{i+8})/(\sum C_{i+1} + C_{i+3} + \ldots + C_{i+9})]$ ratio, with $i = 25$. It can be used as a proxy for the preservation potential of the organic matter when there is a clear predominance of higher plant waxes, that is, due to diagenetic processes their CPI gradually decreases down to 1 (Hedges and Prahl 1993) because of bacterial degradation that produces a same content of odd and even chain alkanes, although CPI may also reflect changes in the contribution from different plant species (Cranwell 1973; Rieley *et al.* 1991; Farrimond and Flanagan 1996; Zhang *et al.* 2004). The values of the CPI proxy in the Villamanrique core (Figure 4a) are between 13.6 (VM-100)

Table 1. ^{14}C dating for sediments from Villamanrique core

Sample	Depth (cm)	Laboratory code	$^{13}C/^{12}C$ ($^0/_{00}$)	Conventional ^{14}C age (ka B.P.)	Calibrated age (ka B.P.)
VM-120	120	Beta-180647	−25.2	1,180 ± 40	1,080 ± 80
VM-378	378	Beta-162117	−25.2	5,100 ± 40	5,830 ± 90
VM-579	579	Beta-180649	−24.5	5,390 ± 40	6,150 ± 130
VM-1703	1703	Beta-162116	−23.9	6,900 ± 40	7,730 ± 70

All samples were analysed in an accelerator mass spectrometer (AMS) in the Beta Analytic Radiocarbon Dating Laboratory (Miami, USA). The ages were calibrated using the INTCAL 98 radiocarbon age calibration program (Stuiver *et al.* 1998).

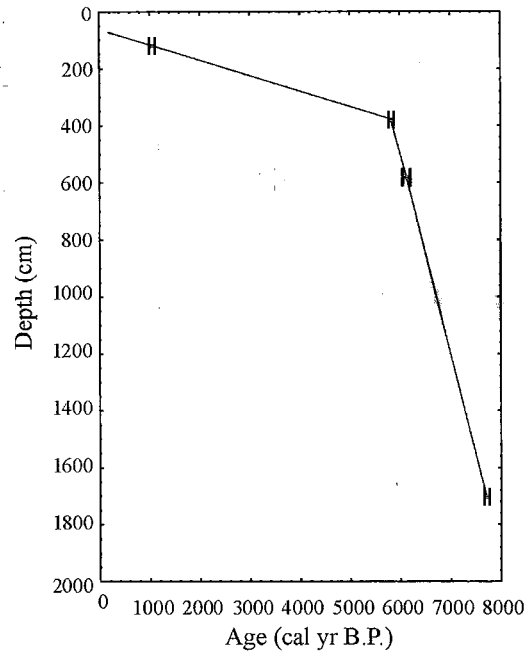

Figure 3. Age-depth relationship for Villamanrique core. Dates (Table 1) have been obtained via the radiocarbon method. Standard deviations for each calibrated age are represented.

and 2.1 (VM-505) and vary only a little between 18.05 and 5.50 m, with a mean value around 7, whereas in the upper 5 m a saw-tooth pattern is observed, with minima at samples VM-1840, VM-505 and VM-450.

The predominant *n*-alkane chain, as well as the *n*-alkane long-chain/short-chain ratio (calculated as $(C_i + C_{i+1} + C_{i+2} \ldots + C_n)/(\sum C_{n+1} + C_{n+2} + \ldots + C_p)$, with $i = 14$, $n = 23$, $p = 37$, based on Duan and Ma (2001) and Xie *et al.* (2003), and the terrigenous/aquatic ratio-TAR_{HC} index (calculated as the $C_{27} + C_{29} + C_{31}/C_{15} + C_{17} + C_{19}$ ratio, defined in Silliman *et al.* (1996), Bourbonniere and Meyers (1996) and Tenzer *et al.* (1999)) can serve as indicators of changes in the terrigenous/aquatic mixture of hydrocarbons, owing to the different *n*-alkane profiles of algae, aquatic macrophytes and vascular plants. In fact, the hydrocarbon distribution of phytoplankton and algae is dominated by low molecular weight *n*-alkanes, maximizing at C_{17} (Gelpi *et al.* 1970; Blumer *et al.* 1971; Cranwell *et al.* 1987). Submerged/floating macrophytes maximize at C_{21}, C_{23} and C_{25} (Cranwell 1984; Ogura *et al.* 1990; Viso *et al.* 1993) as well as many *Sphagnum* species (Bryophyta) (Baas *et al.* 2000; Nott *et al.* 2000; Pancost *et al.* 2002), while emergent macrophytes have *n*-alkane compositions similar to terrestrial plants, that is, maximizing at C_{27} and C_{29} (Cranwell 1984). Terrestrial plants contain high proportions of higher molecular weight *n*-alkanes (C_{27}, C_{29} and C_{31}) in their epicuticular waxy *coatings* (Eglinton and Hamilton 1963, 1967; Eglinton and Calvin 1967; Cranwell *et al.* 1987; Rieley *et al.* 1991; Nott *et al.* 2000; Pancost *et al.* 2002; Liu and Huang, 2001).

Downcore values for the predominant *n*-alkane chain, as well as the *n*-alkane long-chain/short-chain ratio and the terrigenous/aquatic ratio-TAR_{HC} index are shown in Figures 5a and 6a,b. All the samples maximize mainly at C_{31} and C_{29} for the *n*-alkanes (Figure 5a). The *n*-alkane long-chain/short-chain ratio (Figure 6a) provides values greater than 6, except in two cases (VM-1840 and VM-505) and a similar profile is observed in the TAR_{HC} index (Figure 6b) with values higher than 4, with minima at VM-1840, VM-505 and VM-550.

Ficken *et al.* (2000) proposed a proxy (*P*aq index) to determine the submerged/floating aquatic macrophyte input relative to the emergent and terrestrial plant input to lake sediments based on *n*-alkanes of a sample. The profile of the *P*aq index values calculated as the $C_{23} + C_{25}/C_{23} + C_{25} + C_{29} + C_{31}$ ratio (Ficken *et al.* 2000) along the

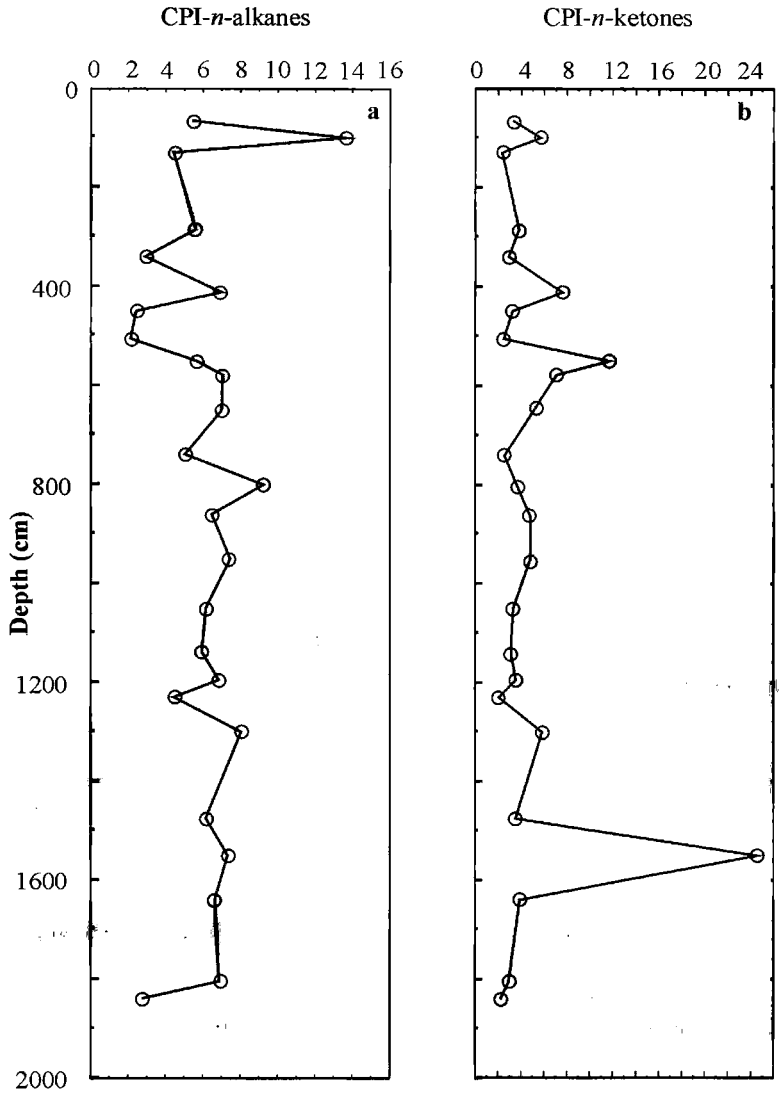

Figure 4. Downcore plots of (**a**) *n*-alkane and (**b**) *n*-ketones CPI values. CPI for *n*-alkanes = $\frac{1}{2}[(\sum C_i + C_{i+2} + \ldots + C_{i+8})/(\sum C_{i-1} + C_{i+1} + \ldots + C_{i+7}) + (\sum C_i + C_{i+2} + \ldots + C_{i+8})/(\sum C_{i+1} + C_{i+3} + \ldots + C_{i+9})]$, with $i = 25$; CPI for *n*-ketones = $\frac{1}{2}[(\sum C_i + C_{i+2} + \ldots + C_{i+8}) + (\sum C_{i+2} + C_{i+2} + \ldots + C_{i+10})/2(\sum C_{i+1} + C_{i+3} + \ldots + C_{i+9})]$, with $i = 21$.

Villamanrique core appear in Figure 6c. Most values are lower or around 0.1, while the highest values of the *P*aq index are observed in samples VM-1840, VM-1230, VM-505 and VM-450.

More specific considerations about the origin of the organic matter can be made by taking into account the distribution of the C_{27}, C_{29} and C_{31} *n*-alkanes (cf. Schwark *et al.* 2002). Typically, grasses and herbs give high concentrations of the C_{31} *n*-alkane, while deciduous tree assemblages, typical of temperate and humid areas, are dominated by the C_{27}-alkane. Conifers, especially pines, are rich in the C_{29} homologue, but also show an important content of the C_{31} *n*-alkane. Rommerskirchen *et al.* (2006) studied the *n*-alkane content in diverse species of grasses and trees in southern Africa, resulting in dominant *n*-C_{31} alkane content in both C_3 and C_4 grasses, while angiosperm C_3 trees maximize at the C_{29} *n*-alkane and in gymnosperm C_3 trees the C_{33} homologue was

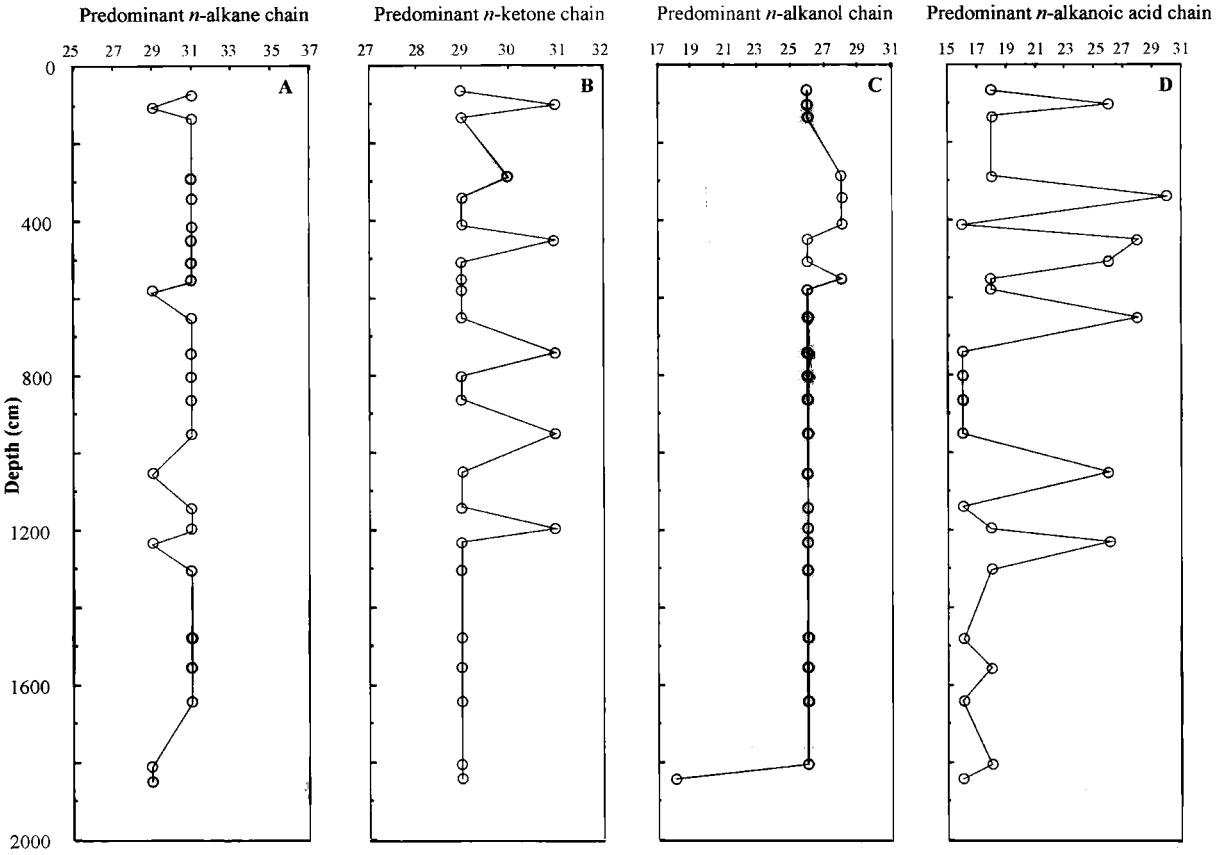

Figure 5. Downcore plots of predominant chain of (**a**) *n*-alkanes, (**b**) *n*-ketones, (**c**) *n*-alkanols and (**d**) *n*-alkanoic acids.

predominant. Analysis of present-day plants of nearby areas to the Villamanrique core performed in our laboratory reveals that deciduous tress maximize at C_{27} *n*-alkane, whereas in herbs the C_{31} *n*-alkane is dominant (cf. Ortiz *et al.* 2004).

Thus, the enrichment in C_{27} *n*-alkane can be attributed to the colonization by many species of deciduous trees and, therefore, the existence of more humid and temperate conditions. On the other hand, high amounts of *n*-C_{31} in sediments can be associated to dry phases, either cold or warm, with the development of an important grass-vegetation cover and/or the development of cold-climate pines.

In this study, we will use the relative percentages of the C_{27}, C_{29} and C_{31} *n*-alkanes is $\%C_i = C_i/100(C_{27} + C_{29} + C_{31})$, with $i = 27, 29$ and 31 (Figure 5d). The percentage of the C_{27} *n*-alkane ranges between 4% (VM-100) and 23% (VM-505), whereas the percentage of the C_{29} homologue is between 33% (VM-450) and 88% (VM-100) and the one for the C_{31} *n*-alkane varies between 12% (VM-100) and 57% (VM-285).

4.3. n-Ketones

n-Ketones, in co-operation with *n*-alkanes and other types of organic compounds, provide information about organic matter sources and their preservation in sediments. Long-chain ketones have several possible origins (Arpino *et al.* 1970; Volkman *et al.* 1981): (a) epicuticular waxes of plants or algae, (b) microbial oxidation of the corresponding *n*-alkanes and (c) microbal β-oxidation and decarboxylation of *n*-fatty acids. When a mismatch in

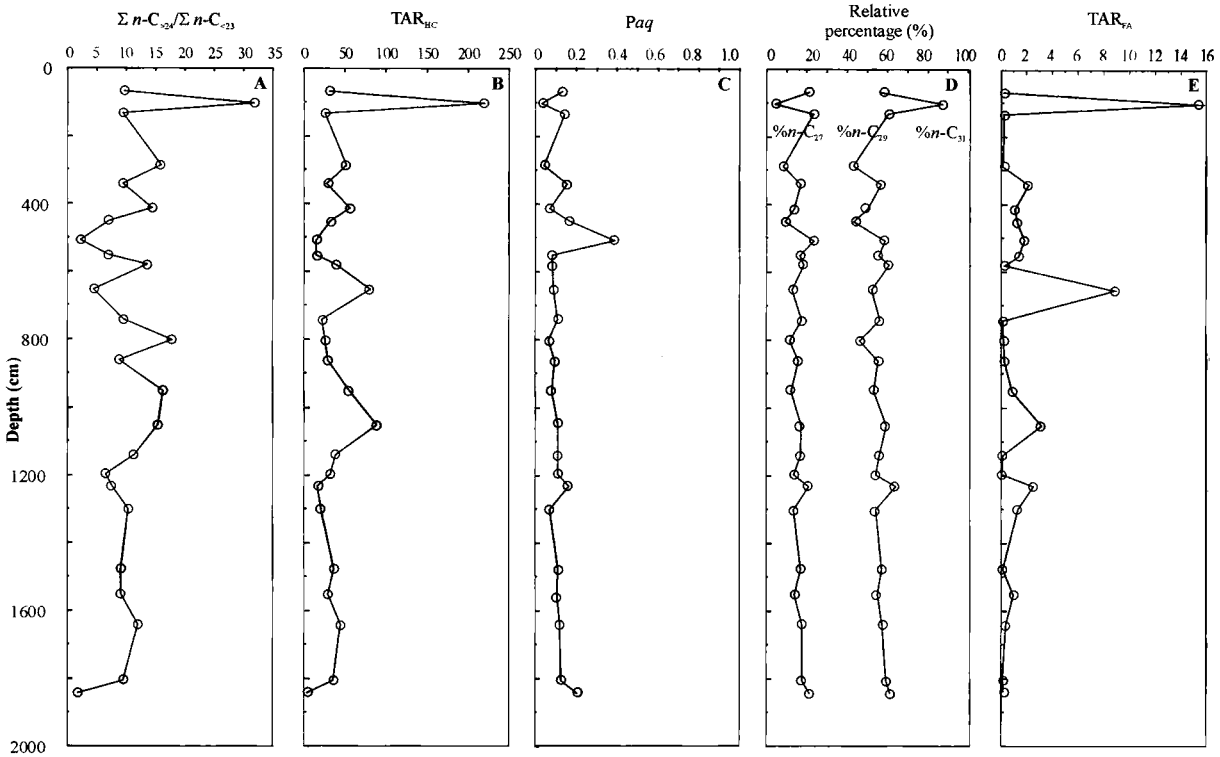

Figure 6. Downcore plots of (**a**) *n*-alkane long-chain/short-chain ratio $[(\sum C_i + C_{i+1} + C_{i+2} \ldots + C_n)/(\sum C_{n+1} + C_{n+2} + \ldots + C_p)$, *with* $i = 14$, $n = 23$, $p = 37]$, (**b**) terrigenous/aquatic ratio for *n*-alkanes: $TAR_{HC} = (C_{27} + C_{29} + C_{31})/(C_{15} + C_{17} + C_{19})$ *n*-alkanes, (**c**) *P*aq index $(C_{23} + C_{25})/(C_{23} + C_{25} + C_{29} + C_{31})$ *n*-alkanes, (**d**) relative percentage of C_{27}, C_{29} and C_{31} *n*-alkane isomers ($\%C_i = C_i/100(C_{27} + C_{29} + C_{31})$ *n*-alkanes, with $i = 27$, 29 and 31) and (**e**) terrigenous/aquatic ratio for *n*-alkanoic acids: $TAR_{FA} = (C_{24} + C_{26} + C_{28})/(C_{14} + C_{16} + C_{18})$ *n*-alkanoic acids.

the CPI between *n*-alkanes and ketones occurs, this indicates that not just microbial oxidation occurred (Xie *et al.* 2003); alternative sources include origins 1 or 3.

The CPI of ketones ($CPI_k = [(\sum C_i + C_{i+2} + \ldots + C_{i+8}) + (\sum C_{i+2} + C_{i+2} + \ldots + C_{i+10})]/2(\sum C_{i+1} + C_{i+3} + \ldots + C_{i+9})$, with$i = 21$) along the Villamanrique core is represented in Figure 4b, whereas the predominant *n*-ketone profile appears in Figure 5b. The values of the CPI_K in the Villamanrique core (Figure 4b) are between 24.6 (VM-1550) and 2.1 (VM-1230). The distribution range of carbon numbers of *n*-ketones is C_{23}–C_{33} and they exhibit odd over even carbon number predominance in all samples, maximizing at C_{29} or C_{31} (Figure 5b).

4.4. n-Alkanols

n-Alkanols provide useful information about organic matter sources and their preservation in sedimentary records and are expected to be at least as bioavailable as the *n*-alkanes (Ficken *et al.* 1998a). They can be used to distinguish between contributions from algae, aquatic macrophytes and land plants to the organic matter preserved in the sediments. Aquatic algae and photosynthetic bacteria contain *n*-alkanols with an even number of carbon atoms ranging from C_{16} to C_{22} (Robinson *et al.* 1984; Volkman *et al.* 1999). A dominance of higher molecular weight *n*-alkanols, C_{22}–C_{30}, with an even carbon predominance, has been ascribed to contributions from epicuticular waxes of land plants (Eglinton and Hamilton 1967; Rieley *et al.* 1991). Individual species of plants often have

distinctive chain length patterns (Ficken *et al.* 1998a,b; Ficken *et al.* 2000) and Rommerskirchen *et al.* (2006) found a general predominance of the C_{32} *n*-alkanol in C_4 plants.

Cyanobacteria and aquatic macrophytes are reported to be major producers of C_{22}–C_{26} *n*-alkanols, with a predominance of *n*-C_{24} (Ficken *et al.* 1998a,b; Volkman *et al.* 1999; Filley *et al.* 2001), and *Sphagnum* species maximize in the C_{24}–C_{28} *n*-alkanols (Baas *et al.* 2000; Pancost *et al.* 2002). Sometimes the *n*-alkanol profile do not correlate well with the corresponding distributions of plants calculated on the basis of pollen counts, which may indicate a preferential microbial attack on the shorter chain homologues (Ficken *et al.* 1998b).

The main distribution range of carbon numbers of *n*-alkanols in Villamanrique core samples is between C_{22} and C_{30}. Nevertheless, there are samples in which the *n*-alkanol profile shows a distribution ranging from the C_{14} isomer to the C_{32} homologue, but in all cases with very low abundances. They have an even-to-odd carbon number predominance, maximizing at C_{26} or C_{28} (Figure 5c), except sample VM-1840, which maximizes at C_{18}.

4.5. n-Alkanoic acids

Like aliphatic hydrocarbons, *n*-alkanoic acid in lake sediments come from organic matter derived from plants and micro-organisms. Long-chain *n*-alkanoic acids (C_{24}–C_{30}), with predominance of even chains, are major components of the waxy coatings on land plant leaves, flowers and pollen (Eglinton and Calvin 1967; Rieley *et al.* 1991; Meyers and Ishiwatari 1993) while algae and bacteria maximize at shorter chain lengths C_{12}–C_{18} (Eglinton and Calvin 1967; Cranwell *et al.* 1987). *Sphagnum* species maximize in the *n*-C_{24} and C_{26} homologues (Baas *et al.* 2000; Pancost *et al.* 2002). In order to calculate the land versus aquatic inputs of organic matter into a lake, Bourbonniere and Meyers (1996) and Tenzer *et al.* (1999) used the terrigenous/aquatic ratio (TAR_{FA}): $(TAR_{FA}) = (C_{24} + C_{26} + C_{28})/(C_{14} + C_{16} + C_{18})$.

Higher values for this ratio indicate increased terrestrial plants relative to aquatic biota, but they can also indicate degradation of aquatic fatty acids relative to land-derived components. Sometimes diagenetic processes can modify TAR_{FA}. Short-chain acids are often preferentially degraded by microbes during early diagenesis (Cranwell 1974, 1976; Haddad *et al.* 1992; Ho and Meyers 1994). On the other hand, microbial synthesis of secondary fatty acids from primary organic matter produces short-chain components (Kawamura *et al.* 1987).

The *n*-alkanoic acids are present in the C_{14}–C_{30} range, with a predominance of even numbered chains and showing a bimodal distribution with maxima at C_{16}–C_{18} or C_{26}–C_{28} (Figure 5d). In some cases the C_{16} and C_{18} homologues are predominant.

4.6. Organic sulphur

Sulphur undergoes cyclic transformations, which can be viewed from different levels of organization and complexity (Jørgensen 1983; Killops and Killops 1984). It is assimilated by most bacteria as well as by algae and other plants in the form of sulphate, which then undergoes an assimilatory reduction via sulphite to sulphide, which is ultimately transferred to amino acids as sulphydryl groups (Siegel 1975). The reduced organic sulphur is again released into the environment after the death and decomposition of the organisms (Jørgensen 1983).

The assimilatory sulphur transformations in living organisms create a cycle between inorganic and organic states of sulphur. In addition, some bacteria can also perform a dissimilatory metabolism of sulphur compounds. These organisms incorporate only a small fraction of the metabolized sulphur into the cells, and most of the sulphur is used in energy metabolism as an electron acceptor or donor in a manner that is similar to the way oxygen is used in aerobic organisms (Jørgensen 1983; Chapman 2001). Some specialized bacteria perform sulphate respiration and release sulphide. Others reoxidize the sulphide, either phototrophically with CO_2 or chemotrophically with O_2 or NO_3^- (Jørgensen 1983; Killops and Killops 1984). In combination, all these different organisms drive the sulphur cycle of ecosystems.

The microbial sulphur cycle begins with the sulphate input into the oceans or palustrine–lacustrine environments that is incorporated into the trophic chain by anaerobic sulphate-reducing bacteria (*Desulphovibrio* sp. and *Desulphobacter* sp. mainly) which perform an assimilatory reduction via sulphite to sulphide (Jørgensen 1983;

Table 2. Correlation coefficients (R) between the relative percentages of C_{27}, C_{29} and C_{31} n-alkanes for Villamanrique core

	$\%C_{29}$	$\%C_{31}$
$\%C_{27}$	−0.1844	−0.9070
	$p = 0.378$	$p = 0.000$
$\%C_{29}$	—	−0.5811
		$p = 0.002$

p: significant level.

5.05 m the values are almost constant, except for the maximum in sample VM-1230, while in the uppermost 5 m the variations are very marked.

To examine the relationship between the relative percentages of C_{27}, C_{29} and C_{31} n-alkanes a multivariate analysis was performed (Table 2), showing a strong negative correlation coefficient between n-C_{27} and n-C_{31} percentages, reflecting different organic matter inputs in the Villamanrique area. This indicates that when the herbaceous vegetation increased in this area it was accompanied with a similar decrease of deciduous trees (high $\%n$-C_{31} and low $\%n$-C_{27}) and *vice-versa*. The percentage of the n-C_{29} alkane shows a negative covariance with the percentage of the n-C_{31} homologue. Although the prevalence of fluvial-derived organic matter detritus is interpreted along the Villamanrique core, the results can be related to the palaeoenvironmental evolution because the catchment area of the Guadiamar River is small and the originally plant remains transported by the river come from the same climatic region, that is, with the same kind of vegetation.

Figure 6d shows slight variations from the bottom of the core to 5.05 m, with values for the C_{27} n-alkane ranging from 12% to 18% and values for the n-C_{31} homologue between 40% and 45%. Values for n-C_{29} are similar to those for n-C_{31}, suggesting a predominance of pine and grass-vegetation. These results coincide with the pollen analysis performed for the Mari-López (cf. Zazo *et al.* 1999; Yll *et al.* 2003) and Marismillas (Yll *et al.* 2003) boreholes, drilled in the Doñana National Park, in which there are monotonous arboreal pollen/non-arboreal pollen values during most of the Holocene (until 2.15 m), suggesting a stable landscape physiognomy. Furthermore, herbaceous taxa and small shrubs are much more abundant than trees, *Pinus* and *Quercus* being the only ones with a significant importance.

Samples VM-950, VM-800 and VM-650 can be highlighted because the percentage of n-C_{31} rises, diminishing both n-C_{27} and n-C_{29} values, which is interpreted as an increase on herbs at the expense of other kinds of plants and, in our opinion, reflects dry episodes. Like the variations in other proxies, samples VM-1840, 1230 and 505 constitute an exception, because the value for the n-C_{27} is over 20% and the n-C_{31} percentage decreases similarly. This suggests a relative rise in rainfall, resulting in the development of deciduous trees.

In contrast with the preceding interval, in the uppermost 5 m there are important oscillations in the relative percentages of n-alkanes (Figure 6d). From 5.05 to 4.50 m (*ca.* 6.0 to 5.9 ka cal. B.P.) the most important colonization of grass vegetation was produced (n-C_{31} % maximum), together with a decline in deciduous tree assemblages (9% of n-C_{27}), which indicates dry conditions and coincides with the end of the post-glacial transgression maximum (Zazo *et al.* 1994; Borrego *et al.* 1999; Dabrio *et al.* 2000).

Between 4.50 and 3.40 m (*ca.* 5.9 to 5.2 ka cal. B.P.) there is a slight decrease in $\%n$-C_{31}, together with a recovery of the $\%C_{27}$ n-alkane, probably linked to a rise in precipitation. This is followed by a decrease in the C_{27} n-alkane to 7.8% in 2.85 m (*ca.* 4.2 ka cal. B.P.), reflecting dry conditions; this coincides with the palaeoenvironmental interpretation of Yll *et al.* (2003) based on pollen analysis of the Doñana National Park boreholes.

At 1.95 m (*ca.* 2.5 ka cal. B.P.) an important increase in n-C_{27}, up to 33%, occurs, with 27% n-C_{31}, which suggests a sharp change in the environmental conditions, probably linked to an augmentation of precipitations, which produced a significant development of deciduous trees.

Sample VM-100 (*ca.* 0.7 ka cal. B.P.) is unusual in that the C_{29} n-alkane contributes 83%, whereas n-C_{27} is around 4% and n-C_{31} is 13%, which indicates an important development of conifers paralleled by a decline in deciduous trees. In the Mari López borehole Zazo *et al.* (1999) observed in the topmost 2.15 m an increase in herbaceous taxa

and the progressive substitution of *Quercus* by *Juniperus* and *Pinus*, which they interpret as the impact of human populations. The values obtained in sample VM-65 suggest more humid conditions. In general, we observed that samples with higher percentages of the C_{27} *n*-alkane present higher *P*aq index values than the general trend, both indicating higher water availability in the area.

The distribution of *n*-ketones observed in seagrass-derived organic matter (Hernández *et al.* 2001) was not found in Villamanrique core sediments. Nor were the *n*-ketone profiles of algae, emergent and submergent plants shown by Wenchuan *et al.* (1999) detected in our chromatograms. Likewise, the long-chain (C_{37}–C_{40}) unsaturated methyl and ethyl ketones, which are mainly produced by haptophyte microalgae in marine waters (Volkman *et al.* 1980, 1995; Rechka and Maxwell 1988) and in coastal and terrestrial habitats (Marlowe *et al.* 1984; Conte *et al.* 1994) were not found.

In any case, the CPI values of *n*-alkanes and *n*-ketones show similar trends (Figure 4a,b). Only in three cases (6.5, 8.0 and 15.5 m) there is a mismatch, in the form of a high increase in the ketone CPI values, which was, in our opinion, due to microbial oxidation and decarboxylation of *n*-fatty acids. Similarly, the predominant *n*-ketone chain profile is similar to the *n*-alkane one (Figure 5a,b), this indicating the possibility of microbial oxidation of *n*-alkanes, which had their origin in terrestrial plants, yielding the corresponding ketones.

The predominant *n*-alkanol chain log (Figure 5c) indicates a major input of land plants (Eglinton and Hamilton, 1967; Rieley *et al.* 1991), which is reinforced by the similar patterns found in the *n*-ketone and *n*-alkane profiles (predominant *n*-alkane and *n*-ketone chains, *n*-alkane long-chain/short-chain ratio, TAR_{HC}: Figure 5a,b; 6a,b).

In contrast, the interpretation of the predominant *n*-alkanoic acid chains (Figure 5d) and TAR_{FA} ratio (Figure 6e, low values) does not corroborate the information obtained from the TAR_{HC} index and other proxies although they all provide, at least in theory, the same information about organic matter origin. Thus, there is a poor covariance between the information provided by the *n*-alkanes, *n*-ketones and *n*-alkanols and that obtained from the *n*-alkanoic acid profiles (see Figure 5a–d; Figure 6b,e). In fact, the *n*-alkanoic acid predominant chain-log shows maxima in either low or high molecular weight homologues (Figure 5d). In all cases, short chain *n*-alkanoic acids are present together with long-chain *n*-alkanoic acids (C_{24}–C_{30}) in the same chromatograms, the latter indicating land plant inputs. Similarly, when the C_{26} and C_{28} isomers are predominant, short chain *n*-alkanoic acids are also present. In our opinion this lack of correspondence can be due to the greater lability of *n*-alkanoic acids to degradation and modification than other lipid biomarkers, such as *n*-alkanes (Meyers and Eadie 1993). In fact, they are usually more useful as indicators of the amounts of organic matter recycling in lake sediments than as recorders of the original sources of organic matter.

In brief, the difference between the profiles of *n*-alkanes and *n*-alkanoic acids (Figure 5a,d) probably reflects a combination of continual microbial degradation and resynthesis of fatty acids in the sediment and partial replacement of originally deposited fatty acids by secondary, microbial fatty acids (Tenzer *et al.* 1999; Xie *et al.* 2003), and usually produces a predominance of short-chain components (Kawamura *et al.* 1987).

The organic sulphur log (Figure 7a) indicates the existence of two main zones in the core, from *ca.* metre 5 to the bottom of the core with presence of organic sulphur, and the uppermost part, lacking this compound. As one of the main requirements for the activity of the sulphate-reducing bacteria is the presence of sulphate ions, together with reducing conditions (Jørgensen 1983; Bondeau and Westrich, 1984), we interpret the huge drop observed in the uppermost 5 m as the transition from marine to freshwater conditions in this area caused by the predominance of fluvial input, that is, with a lower sulphate supply, bacterial sulphate reduction, should decrease in an important way.

In fact, Bates *et al.* (1984) interpreted changes in sulphur content with depth in cores from the Everglades (Florida) as changes in sulphur loading over time, which in turn, depend mainly on the dissolved sulphate content input, but also on the microbial activity and redox potential (Berner, 1984). This might also indicate the existence of a relatively important water column, producing stratification with a prevalence of anoxic conditions, from the bottom of the core to 3.40 m, with the exception of sample SVM-505. According to Cabrera *et al.* (2002), a high sulphur content in sediments reflects a very active sulphur cycling which is mainly related to sulphate-reducing bacteria, but also involves anaerobic photosynthetic sulphur bacteria and, therefore, reducing conditions.

In our opinion, the organic sulphur content of the Villamanrique borehole (Figure 7a) is a good reliable proxy for reflecting fluvial input and the oxic/anoxic conditions.

Wang X-C, Chen RF, Berry A. 2003. Sources and preservation of organic matter in Plum Island salt marsh sediments (MA, USA): long-chain n-alkanes and stable carbon isotope compositions. *Estuarine, Coastal and Shelf Science* **58**: 917–928.

Wenchuan Q, Dickman M, Sumin W, Ruijin W, Pingzhong Z, Jianfa C. 1999. Evidence for an aquatic plant origin of ketones found in Taihu Lake sediments. *Hydrobiologia* **397**: 149–154.

Xie S, Lai X, Yi Y, Gu Y, Liu Y, Wang X, Liu G, Liang B. 2003. Molecular fossils in a Pleistocene river terrace in southern China related to paleoclimate variation. *Organic Geochemistry* **34**: 789–797.

Yll R, Zazo C, Goy JL, Pérez-Obiol R, Pantaleón-Cano J, Civis J, Dabrio C, González A, Borja F, Soler V, Lario J, Luque L, Sierro F, González-Hernández FM, Lezine AM, Denefle M, Roure JM. 2003. Quaternary palaeoenvironmental changes in south Spain. In *Quaternary Climatic Changes and Environmental Crises in the Mediterranean Region*, Ruiz Zapata MB, Dorado Valiño M, Valdeolmillos Rodríguez A, Gil García MJ, Bardají Azcárate T, De Bustamante Gutiérrez I, Martínez Mendizábal I (eds). Universidad de Alcalá de Henares: Alcalá de Henares; 201–213.

Yuan F, Linsley BK, Howe SS, Lund SP, McGeehin JP. 2006. Late Holocene lake-level fluctuations in Walker Lake, Nevada, USA. *Palaeogeography, Palaeoclimatology, Palaeoecology* **240**: 497–507.

Zazo C, Goy JL, Somoza L, Dabrio CJ, Belluomini G, Improta S, Lario J, Bardaji T, Silva PG. 1994. Holocene sequence of sea-level fluctuations in relation to climatic trends in the Atlantic-Mediterranean linkage coast. *Journal of Coastal Research* **10**: 933–945.

Zazo C, Dabrio CJ, González A, Sierro F, Yll EI, Goy JL, Luque L, Pantaleón-Cano J, Soler V, Roure JM, Lario J, Hoyos M, Borja F. 1999. The record of the latter glacial and interglacial periods in the Guadalquivir marshlands (Mari López drilling, S.W. Spain). *Geogaceta* **26**: 119–122.

Zhang Z, Zhao M, Yang X, Wang S, Jiang X, Oldfield F, Eglinton G. 2004. A hydrocarbon biomarker record for the last 40 kyr of plant input to Lake Heqing, southwestern China. *Organic Geochemistry* **35**: 595–613.